The Madden_Julian Oscillation and its Impact on Northern Hemisphere Weather Predictability during Wintertime

Charles Jones

Institute for Computational Earth System Science

University of California, Santa Barbara, California, USA

Duane E. Waliser

Institute for Terrestrial and Planetary Atmospheres

State University of New York, Stony Brook, New York

K. M. Lau

Climate and Radiation Branch,

Goddard Space Flight Center, NASA, Greenbelt, MD

W. Stern

Geophysical Fluid Dynamics Laboratory

Princeton University, Princeton, NJ

Corresponding author address: Dr. Charles Jones, Institute for Computational Earth

System Science, University of California, Santa Barbara, CA 93106, USA.

Email: cjones@icess.ucsb.edu

Abstract

The Madden-Julian Oscillation (MJO) is known as the dominant mode of tropical intraseasonal variability and has an important role in the coupled-atmosphere system. This study used twin numerical model experiments to investigate the influence of the MJO activity on weather predictability in the midlatitudes of the Northern Hemisphere during boreal winter. The National Aeronautics and Space Administration (NASA) Goddard laboratory for the Atmospheres (GLA) general circulation model was first used in a 10-yr simulation with fixed climatological SSTs to generate a validation data set as well as to select initial conditions for active MJO periods and Null cases. Two perturbation numerical experiments were performed for the 75 cases selected [(4 MJO phases + Null phase) _ 15 initial conditions in each]. For each alternative initial condition, the model was integrated for 90 days. Mean anomaly correlations in the midlatitudes of the Northern Hemisphere (20°N_60°N) and standardized root-mean-square errors were computed to validate forecasts and control run. The analyses of 500-hPa geopotential height, 200-hPa Streamfunction and 850-hPa zonal wind component systematically show larger predictability during periods of active MJO as opposed to quiescent episodes of the oscillation.

1. Introduction

The Madden-Julian Oscillation (MJO) is known as the dominant mode of tropical intraseasonal variability with characteristic time scales of 30_60 days (Madden and Julian 1994). The MJO is typically quite active in the boreal winter and is characterized by significant equatorial eastward propagation (Jones et al. 2002). The influences of the MJO on the patterns of large-scale circulation and precipitation in the global tropics and in portions of the extratropics have been well documented. For example, the MJO strongly influences the precipitation patterns associated with the monsoons in Asia, Australia, North America and South America (Yasunari 1979; Lau and Chan 1986; Kiladis and Weickmann 1992; Mo and Higgins, 1998; Mo 2000; Nogués-Paegle et al 2000; Higgins et al. 2000; Higgins and Shi 2001; Jones and Carvalho 2002). Additionally, this influence has been shown to modulate rainfall variability and extreme events in the Americas as well (Higgins et al. 2000; Jones 2000; Carvalho et al. 2003).

Specifically with respect to the strength of the MJO and/or the accuracy of its representation in numerical weather forecast models, the study of Ferranti et al. (1990) suggested that the predictive skill of medium-to-extended range forecasts in the Pacific North American region are significantly improved when the errors associated with the representation of the MJO are minimized. In another study, Lau and Chang (1992) analyzed one season of 30-day global forecasts derived from the National Centers for Environmental Prediction (NCEP) forecast model during the Dynamical Extended Range Forecasts (DERF) experiment. Their results showed that the NCEP forecast model has skill in predicting the global pattern of intraseasonal variability up to 10 days, with the error growth of tropical and extratropical low-frequency modes less (greater)

than persistence when the amplitude of the MJO is large (small). Using a more recent version of DERF experiments, Hendon et al. (2000) found that forecasts in the Tropics and midlatitudes of the Northern Hemisphere during boreal winter have less skill when they are initialized during or prior to periods of active MJO as opposed to quiescent episodes of the oscillation. They attributed the reduced forecast skill to the inability of the numerical model to sustain the MJO beyond about 7 days, which contribute to erroneous tropical Rossby wave sources. Likewise, skills of medium range weather forecasts in the Pan American sector have also been linked to tropical intraseasonal variability (Nogués-Paegle et al., 1998). Jones and Schemm (2000) used NCEP/DERF90 experiments to investigate the influence of the MJO variability in numerical weather forecasts over South America. The results indicated more skill during periods of strong convective activity associated with the MJO as opposed to periods of suppressed or weak activity.

A key aspect in the issue of investigating the MJO impacts on extratropical weather variability is that the previous studies have used global numerical models with notably poor/weak representations of the MJO (Lau and Chang, 1992; Hendon et al. 2000; Jones et al 2000). Furthermore, previous studies that have addressed the impact of MJO variability have done so by assessing forecast skill rather than by examining its effects on midlatitudes predictability (Lau and Chang, 1992; Hendon et al. 2000). The two issues above together with large errors present in tropical initial conditions unable to derive definite conclusions about the influence of the MJO on midlatitudes weather predictability. Motivated by these reasons, this study uses a set of twin predictability experiments to investigate the following question: *What is the overall influence of MJO*

activity on weather predictability in the northern hemisphere midlatitudes during boreal winter?

2. Model

In order to investigate the influence of the MJO on midlatitudes weather predictability, this study uses the exact same model described in Waliser et al. (2003a,b). The numerical model is the National Aeronautics and Space Administration (NASA) Goddard laboratory for the Atmospheres (GLA) general circulation model (GCM), which an earlier version is described in Kalnay et al. (1983). Modifications have included increased vertical resolution and several changes in the parameterizations of radiation, convection, cloud formation, precipitation, vertical diffusion, and surface processes (Sud and Walker 1992; Phillips 1996). The horizontal representation uses surface finite differences on a 4° _ 5° (latitude _ longitude) energy and momentum conserving A grid (Arakawa and Lamb 1977). The vertical domain has 17 unequally spaced sigma levels extending from the surface to about 12 hPa. Both seasonal and diurnal cycles in the solar forcing are simulated with the atmospheric radiation treatment of Harshvardhan et al. (1987). The formulation of convection follows the scheme of Arakawa and Schubert (1974), as implemented in discrete form by Lord and Arakawa (1980). The model orography is based on the 1°ᵡ 1° topographic height data of Gates and Nelson (1975), which has been area averaged over the 40 _ 50 grid boxes. The resulting orography is smoothed using a 16th-order Shapiro (1970) filter, and a Fourier filter poleward to 60° latitude.

In general, the GLA model performed very well with respect to its representation of the MJO in the Slingo et al. (1996) Atmospheric Model Intercomparison Project

(AMIP) study. Further comparison by Sperber et al. (1996) revealed that the GLA, along with the United Kingdom Meteorological Office (UKMO) model and version 2 of the Community Climate Model (CCM2), exhibited variability closely resembling the observed features of the MJO. In particular, the GLA model tended to produce a better representation of the eastward propagation of convection and its associated cyclonic and anticyclonic circulation anomalies when compared to the UKMO model. As a first assessment of the MJO influence on midlatitudes weather predictability, this study utilizes the fixed SST version of the model, although simulations with interactive SST by means of a slab-ocean showed some modest improvements in the GLA simulation of the MJO (Waliser et al. 1999).

3. Experimental Framework

The experimental approach followed to examine the MJO influence on weather predictability during extended boreal winter (November – April) was determined using a set of twin predictability experiments (Waliser et al. 2003a). Initial conditions for a number of MJO events were first determined by performing a 10-yr simulation using climatological SSTs. Daily averages (four 6-h values) of a number of fields were saved. From this simulation, MJO events were chosen based on an extended empirical orthogonal function analysis (EEOF) of rainfall data from the region 32°N–32°S and 32.5°E–92.5°W. This region tends to encompass most of the variability in rainfall that is associated with the MJO (e.g., Lau and Chan 1986; Wang and Rui 1990). To isolate the intraseasonal timescale, and thus the MJO, the data were first bandpassed with a 30–90-day Lanczos filter (Duchon 1979). EEOF analysis, using temporal lags from −7 to

+7 pentads, was then performed on pentad averages. The first (second) mode contains 6.0% (5.9%) of the variance of the time-lagged sequences of the bandpassed data.

Candidate MJO events to use for initial conditions were chosen from the amplitude time series associated with model EEOF modes 1 and 2. Given that these modes capture the propagating nature of the MJO, selecting periods when the amplitude of these time series is large will tend to capture strong, propagating MJO events. The two series have maximum correlation (0.95) at a lag of +/– ~ 12 days, indicating a dominant period of about 50 days. When the mode-1 time series is positive (negative), rainfall tends to be high in the western Indian (western Pacific) Ocean, and when the mode-2 time series is positive (negative), rainfall tends to be high in the eastern Indian (central Pacific Ocean/South Pacific convergence zone) Ocean (see Waliser et al. 2003a). Thus, by selecting periods of both positive and negative values of these two series, four separate "phases" of the MJO can be distinguished based on the longitudinal position of the heating.

For each of these four phases, the 15 events with the greatest amplitudes for each of the four phases were selected. In order to contrast the difference in midlatitudes weather atmospheric predictability between periods of high MJO activity to those with little or no MJO activity, 15 initial conditions were also chosen from periods in which neither of the above modes, nor their Northern Hemisphere (NH) "summertime" (May–October) counterpart, were strongly exhibited in the model atmosphere. The selection was performed as follows. The amplitude time series for EEOF modes 1–4 for the Northern Hemisphere winter, along with the analogous four series for the summer, were squared, added together, and then smoothed with a 51-day (~ MJO cycle) running

filter. This combined series gives a bulk index of generalized intraseasonal activity. The 15 events during boreal winter with the lowest values of this index were selected to represent low MJO activity conditions with the additional criteria that the events had to occur at least 10 days apart. The latter criterion was applied in order to get a sample of distinct atmospheric states of low MJO activity (see Waliser et al. 2003 for details). Hereafter, these cases will be referred to as Null events. Figure 1 shows the composites of rainfall for the 15 initial conditions selected for each of the four MJO phases (indicated as Indian, Maritime, W. Pacific and C. Pacific) as well as the Null events.

Two perturbations were performed for the 75 cases selected [(4 MJO phases + Null phase) _ 15 events]. The perturbation initial conditions were determined as follows. Given the day of the month that the initial condition occurs, day-to-day root-mean-square (rms) differences were computed (on the model's sigma surfaces) from the daily averaged values of the model's four prognostic variables (u,v,T,q) for that particular month. This process was meant to provide some spatial structure to the perturbation, whereby larger day-to-day variability would translate into more uncertainty in the initial conditions. These rms values were then multiplied by a random number scaled between −0.1 and 0.1 for the first set of perturbations and −0.2 and 0.2 for the second set. These "errors" were then added to the original initial condition's prognostic values to produce an alternative initial condition. The different size error between the first set and second set will be used to provide some information on the sensitivity of the midlatitudes weather predictability to the size of the initial condition perturbation. For each alternative initial condition, the model was integrated for 90 days.

4. Results

The influence of the MJO on boreal winter weather predictability was examined in the following model's variables: 500-hPa geopotential height (Z500), 200-hPa Streamfunction (SF200), 850-hPa zonal wind component (U850) and rainfall. Daily anomalies of each of these variables were calculated by subtracting the seasonal cycle determined from the 10-yr fixed SST climatological run. No other filtering was applied to the time series. In the remainder of this section, we contrast the predictability obtained during periods of high MJO activity (120 events: 4 phases x 15 cases x 2 perturbations) with low intraseasonal activity or Null cases (30 events: 15 cases x 2 perturbations).

A number of ways have been proposed to assess forecast skill (Miller and Roads 1990; Déqué and Royer 1992; Wilks 1995). In this study, mean anomaly correlation (or pattern correlation) was computed as:

$$\text{Mean ACC} = \frac{\overline{\langle (O')(F') \rangle}}{\left[\overline{\langle (O')^2 \rangle \langle (F')^2 \rangle} \right]^{1/2}} \tag{1}$$

where O' is the "observed" daily anomaly from the 10-yr climatological run and F' is the daily anomaly forecast. Brackets indicate the integration over the spatial domain. Although there are different ways of computing mean acc (Déqué and Royer 1992), the arithmetic mean over the sample size is used in this work, which is denoted by overbars. The sample size can be 120 for all MJO cases, 30 for each MJO phase and 30 for Null cases. In addition, the expression above was calculated for lead times from 1 to 30 days.

Figure 2 shows the mean acc of Z500, SF200 and U850 computed over the Northern Hemisphere midlatitudes (20°N_60°N). A common feature shown in the

computation of mean acc is the systematically lower predictability obtained during periods of quiescent MJO. For instance, the mean acc of Z500 reaches a value of 0.6 at 15 days lead time during Null cases, whereas the mean acc extends to about 16_18 days lead times during active MJO. In particular, the MJO phase denoted by INDIAN, which corresponds to increased precipitation in the western Indian and central Pacific Oceans (Fig. 1), shows the largest mean acc for all three variables.

In order to inspect case-to-case variations and assess the robustness of the twin set of predictability experiments, Fig. 3 displays the acc of Z500 (20°N_60°N) for each case and perturbation initial conditions contained in the INDIAN MJO phase (left column) and Null sample (right column) at 5, 10, 15 and 20 days lead time. The horizontal lines indicate the mean acc over all cases at the given lead time. The important point to note is that, in general, the acc is uniformly distributed across the cases for both INDIAN MJO and Null situations and therefore not influenced by only a few cases.

An estimate of the statistical significance of differences in mean acc between active MJO and Null cases was achieved with the following procedure. The Fisher transformation (Γ) was first applied to the mean acc at each lead time to ensure a more Gaussian distribution than the mean acc given by (1) (Miller and Roads 1990; Wilks 1995):

$$\Gamma(\tau) = 0.5 \ln \frac{(1 + \rho)}{(1 - \rho)} \tag{2}$$

where ρ is the mean acc at the lead time τ. Next, the test statistic Z was computed for the differences between Γ in active MJO phases and Null cases at each lead time:

10

$$\text{Æ} = \frac{(\Gamma_{MJO} - \Gamma_{Null})}{\sqrt{\dfrac{\acute{O}^2_{MJO}}{N_{MJO}} - \dfrac{\acute{O}^2_{Null}}{N_{Null}}}} \tag{3}$$

where σ is the variance of Γ and N the number of cases. Figure 4 shows the Z statistic at lead times from 10 to 15 days for Z500, SF200 and U850 and each MJO phase. Values of Z greater than 1.96 (1.64) indicate that differences in Γ are statistically significant at 95% (90%) level. Thus, the results based on mean acc suggest higher weather predictability in the Northern Hemisphere midlatitudes during the active INDIAN phase of MJO relative to quiescent episodes of the oscillation.

Another way of estimating predictability is by computing the root-mean-square (rms) error between "observations" (10-yr fixed SST climatological run) and forecast fields. Since the variance during periods of active MJO and Null situations can be significantly different in the midlatitudes of the Northern Hemisphere, a standardized rms error was computed. This was accomplished by normalizing each time series of observation and forecast by the mean and standard deviation of the climatological run time series encompassing each initial condition for each case and perturbation (i.e. 30 days before and 90 days after a given initial condition). Figure 5 shows the standardized rms error, spatially averaged from 20°N to 60°N, for the fields of Z500, SF200 and U850. Higher predictability is obtained during active MJO situations than in the Null cases. In agreement with results shown before, the INDIAN phase associated with active MJO cases exhibits the highest skill. For example, while the standardized rms error in Z500 reaches a value of 1 at 15 days lead time in the Null cases, the rms error attains a value of 1 at about 18 days lead time during the INDIAN phase.

The influence of the MJO on boreal winter weather predictability was further investigated by examining the mean acc between "observed" and forecasted rainfall during active MJO and Null cases. Three domains (Fig. 6) were chosen: tropical Indian Ocean and western Pacific, western North America and eastern South America. These regions were selected given that observational studies have related the eastward propagation of the MJO with significant changes in rainfall in those areas (Yasunari 1979; Lau and Chan 1986; Mo 2000; Nogués-Paegle et al 2000; Higgins and Shi 2001; Jones and Carvalho 2002; Higgins et al. 2000; Jones 2000; Carvalho et al. 2003). Figure 6 displays the mean acc for rainfall over the selected regions. It is interesting to note that there are not major differences in mean acc during active MJO and quiescent periods, which perhaps results from the stochastic nature of rainfall variability.

5. Summary and Conclusions

This study used twin numerical model experiments to investigate the influence of the MJO activity on weather predictability in the midlatitudes of the Northern Hemisphere during boreal winter. The NASA_GLA general circulation model was first used in a 10-yr simulation with fixed climatological SSTs to generate a validation data set as well as to select initial conditions for active MJO periods and Null cases. Two perturbation numerical experiments were performed for the 75 cases selected [(4 MJO phases + Null phase) _ 15 initial conditions in each]. For each alternative initial condition, the model was integrated for 90 days. Mean anomaly correlations in the midlatitudes of the Northern Hemisphere (20°N_60°N) and standardized root-mean-square errors were computed to validate forecasts and control run. The analyses of Z500, SF200 and U850 fields systematically show larger predictability during periods of

12

active MJO as opposed to quiescent episodes of the oscillation. These results are in agreement with the increased predictive skill obtained during situations of amplified tropical intraseasonal variability discussed by Ferranti et al. (1990) and Lau and Chang (1992).

There are a number of caveats that should be noted. First, while the intraseasonal peak of equatorial wavenumber_1, upper-level velocity potential and zonal wind for the model is quite similar, in terms of magnitude and frequency, to observations, the model spectra has too much high-frequency (~days) variability for wavenumber_1 (Slingo et al. 1996). Relative to the MJO, this variability would be considered to be unorganized, errant convective activity that may erode the relatively smooth evolution of the MJO. Second, these simulations were carried out with fixed climatological SST values. A previous study with this model showed that coupled SSTs tend to have an enhancing and organizing influence on the MJO, making it stronger and more coherent (Waliser et al. 1999). The third aspect is the fact that the model contains too little variability over the western Indian Ocean and southern Maritime Continent region. It is interesting to observe, however, that the MJO phase corresponding to enhanced precipitation in the Indian and western Pacific Oceans (INDIAN) is associated with the largest predictability sensitivity found with this numerical model. Further experiments are necessary to better identify the exact location of enhanced tropical precipitation associated with active MJO that have the largest impact for weather predictability. In this regard, the importance of the MJO modulating weather predictability during boreal summer has also been investigated using the NASA_GLA model, although this modulation is not conclusive.

Observational studies have extensively indicated a significant role of the MJO on rainfall variability in the Tropics and extratropical regions of the Americas. While the predictability experiments shown here indicate an MJO impact on boreal winter large-scale circulation (Z500, SF200 and U850), the influence of active MJO periods on rainfall predictability is less clear (Fig. 6). Our current research is examining this topic further, including a possible modulation of the MJO on the predictability of extreme rainfall events.

References

Arakawa, A., and W. H. Schubert, 1974: Interaction of a cumulus cloud ensemble with the large-scale environment. Part I. *J. Atmos. Sci.,* **31,** 674–701.

Carvalho, L. M., C. Jones, and B. Liebmann, 2003: The South Atlantic Convergence Zone: persistence, intensity, form, extreme precipitation and relationships with intraseasonal activity. *J. Climate* (in revision).

Déqué, M., and J. F. Royer, 1992: The skill of extended-range extratropical winter dynamical forecasts. *J. Climate,* **5,** 1346-1356.

Duchon, C. E., 1979: Lanczos filter in one and two dimensions. *J. Appl. Meteor.,* **18,** 1016–1022.

Ferranti, L., T. N. Palmer, F. Molteni and K. Klinker, 1990: Tropical-extratropical interaction associated with the 30-60 day oscillation and its impact on medium and extended range prediction. *J. Atmos. Sci.,* **47,** 2177-2199.

Gates, W. L., and A. B. Nelson, 1975: A new (revised) tabulation of the Scripps topography on a one-degree global grid. Part 1: Terrain heights. Tech. Rep. R-1276-1-ARPA, The Rand Corporation, Santa Monica, CA, 132 pp.

Hendon, H. H., B. Liebmann, M. Newman, J. D. Glick, and J. Schemm, 2000: Medium range forecast errors associated with active episodes of the Madden–Julian oscillation. *Mon. Wea. Rev.,* **128,** 69–86.

Higgins, R. W., J.-K. E. Schemm, W. Shi, A. Leetmaa, 2000: Extreme Precipitation Events in the Western United States Related to Tropical Forcing. *J. Climate,* **13,** 793–820.

Higgins, R. W., and W. Shi, 2001: Intercomparison of the principal modes of interannual and intraseasonal variability of the North American monsoon system. *J. Climate,* **14**, 403-417.

Jones, C., and L. M. V. de Carvalho, 2002: Active and break phases in the South American Monsoon System. *J. Climate*, **15**, 905-914.

————, L. M. V. Carvalho, W. Higgins, D. Waliser, J-K. Schemm, 2002: Climatology of Tropical Intraseasonal Convective Anomalies: 1979-2002. . *J. Climate (in revision).*

————, 2000: Occurrence of extreme precipitation events in California and relationships with the Madden–Julian oscillation. *J. Climate,* **13**, 3576–3587.

————, D. E. Waliser, J. K. Schemm, and W. K. Lau, 2000: Prediction skill of the Madden–Julian oscillation in dynamical extended range forecasts. *Climate Dyn.,* **16**, 273–289.

————, and J.-K. E. Schemm, 2000: The influence of intraseasonal variations on medium-range weather forecasts over South America. *Mon. Wea. Rev.,* **128**, 486–494.

Kalnay, E., R. Balgovind, W. Chao, D. Edelmann, J. Pfaendtner, L. Takacs, and K. Takano, 1983: Documentation of the GLAS fourth-order general circulation model. Vol. 1. NASA Tech. Memo. 86064,NASA Goddard Space Flight Center, Greenbelt, MD, 436 pp.

Kiladis, G. N., and K. M. Weickmann, 1992: Circulation anomalies associated with tropical convection during Northern winter. *Mon. Wea. Rev.,* **120**, 1900-1923.

Lau, K. M. and P. H. Chan, 1986: Aspects of the 40-50 Day oscillation during the Northern Summer as inferred from Outgoing Longwave Radiation. *Mon. Wea. Rev.*, **114**, 1354-1367.

Lau, K. M. and F. C. Chang, 1992: Tropical intraseasonal oscillation and its prediction by the NMC operational model. *J. Climate*, **5**, 1365-1378.

Lord, S. J., and A. Arakawa, 1980: Interaction of a cumulus cloud ensemble with the large-scale environment. Part 2. *J. Atmos. Sci.*, **37**, 2677–2962.

Madden, R. A., and P. R. Julian, 1994: Observation of the 40–50-day tropical oscillation—A review. *Mon. Wea. Rev.*, **122,** 814–837.

Miller, A. J., and J. O. Roads, 1990: A Simplified Coupled Model of Extended-Range Predictability. *J. Climate,* **3**, 523–542.

Mo, K. C., 2000: Intraseasonal modulation of summer precipitation over North America. *Mon. Wea. Rev.*, **128**, 1490-1505.

Nogués-Paegle, J., L. A. Byerle, and K. Mo, 2000: Intraseasonal modulation of South American summer precipitation. *Mon. Wea. Rev.,* **128**, 837-850.

_____, K. Mo, and J. Paegle, 1998: Predictability of the NCEP-NCAR reanalysis model during austral summer. *Mon. Wea. Rev.*, **126**, 3135-3152.

Phillips, T. J., 1996: Documentation of the AMIP models on the World Wide Web. *Bull. Amer. Meteor. Soc.,* **77,** 1191–1196.

Shapiro, R., 1970: Smoothing, filtering and boundary effects. *Rev. Geophys. Space Phys.,* **8,** 359–387.

Slingo, J. M., and Coauthors, 1996: Intraseasonal oscillations in 15 atmospheric general circulation models: Results from an AMIP diagnostic subproject. *Climate Dyn.*, **12,** 325–357.

Sperber, K. R., J. M. Slingo, P. M. Inness, and K.-M. Lau, 1996: On the maintenance and initiation of the intraseasonal oscillation in the NCEP/NCAR reanalysis and the GLA and UKMO AMIP simulations. *Climate Dyn.,* **13,** 769–795.

Sud, Y. C., and G. K. Walker, 1992: A review of recent research on improvement of physical parameterizations in the GLA GCM. *Physical Processes in Atmospheric Models,* D. R. Sikka and S. S. Singh, Eds., Wiley Eastern Ltd., 422–479.

Waliser, D. E., K. M. Lau, W. Stern, C. Jones, :2003a: Potential predictability of the Madden-Julian Oscillation. *Bull. Amer. Meteo. Soc.*, 33-50.

_____, W. Stern, S. Schubert, and K. M. Lau, 2003b: Dynamic predictability of intraseasonal variability associated with the Asian summer monsoon. *Quart. J. Roy. Meteor. Soc.* (accepted).

_____, K. M. Lau, and J.-H. Kim, 1999: The influence of coupled sea surface temperatures on the Madden–Julian oscillation: A model perturbation experiment. *J. Atmos. Sci.,* **56,** 333–358.

Wang, B., and H. Rui, 1990: Synoptic climatology of the transient tropical intraseasonal convection anomalies. *Meteor. Atmos. Phys.,* **44,** 43–61.

Wilks, D. S., 1995: *Statistical Methods in the Atmospheric Sciences.* Academic Press, 464 pp.

Yasunari, T., 1979: Cloudiness fluctuations associated with the Northern Hemisphere monsoon. *J. Met. Soc. Japan.*, **58,** 225-229.
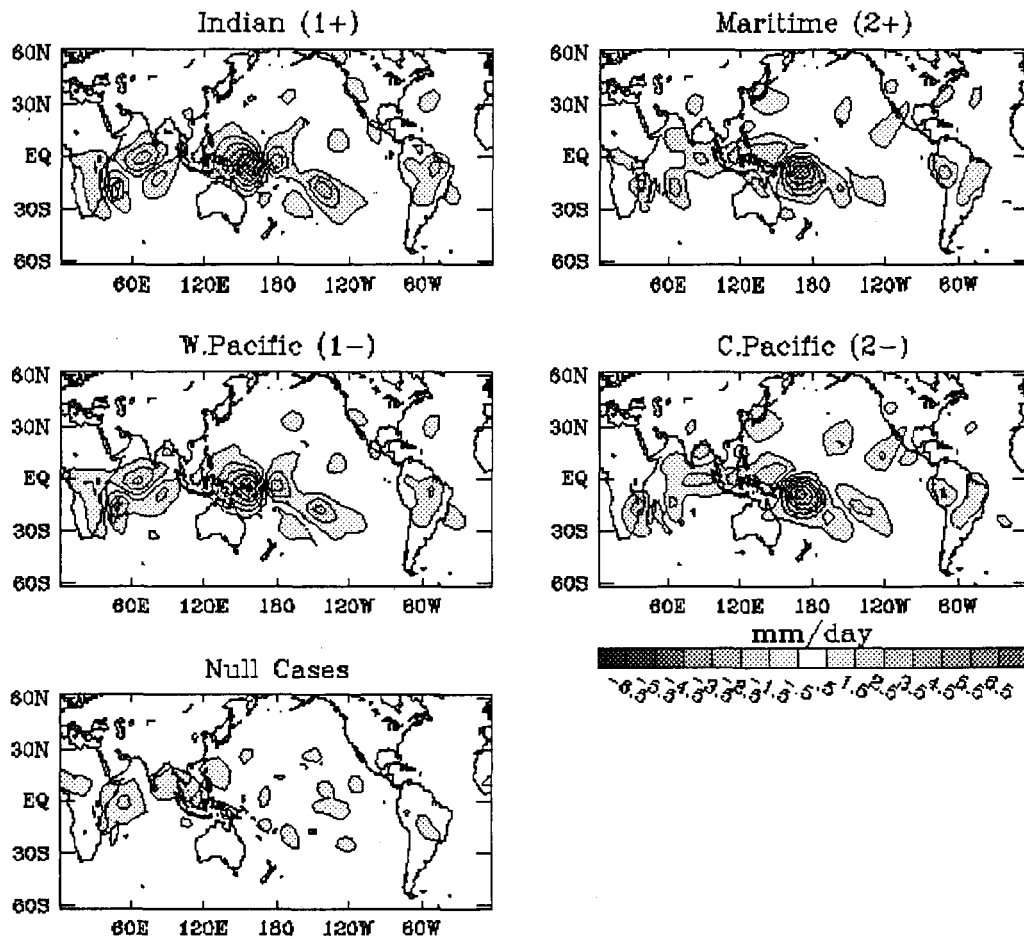
Figure 1. Composite of filtered (30-90 days) rainfall anomalies for the 15 initial conditions selected to represent the four "phases" of the MJO (upper four panels) as well as the Null cases (lower panel). For example, the upper left panel [i.e. Indian (1+)] is the average rainfall anomaly from the fifteen initial conditions derived from the largest positive amplitudes of the first time series of EEOF analysis (similarly, for the other panels). Except in the Null case (lower left), the headings indicate the geographic region of the most intense MJO-related rainfall as well as the rainfall EEOF mode and sign (e.g., 1+ indicates EEOF mode 1 > 0).
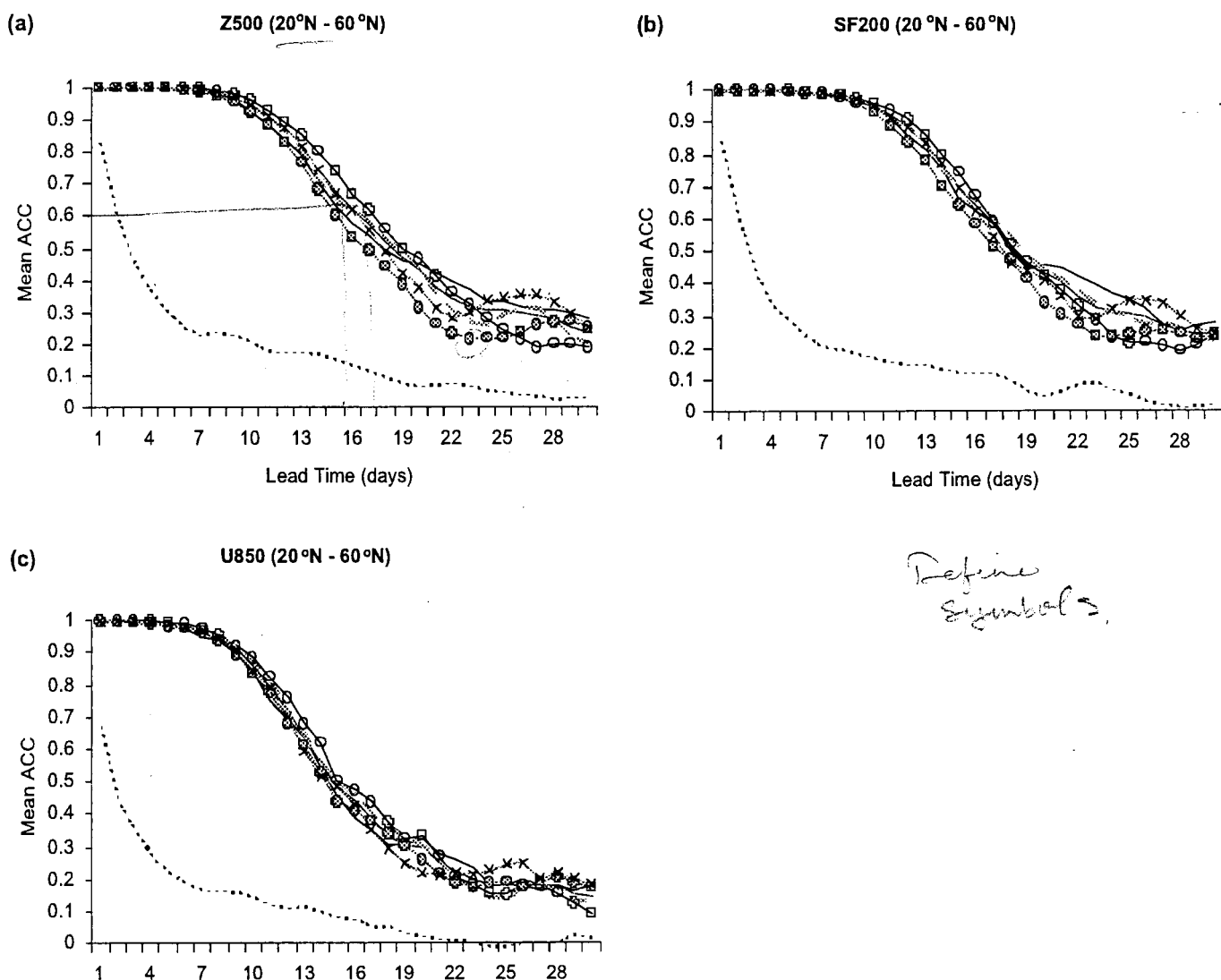
(a) Z500 (20°N - 60°N)

(b) SF200 (20 °N - 60°N)

(c) U850 (20 °N - 60°N)

Figure 2. Boreal winter mean anomaly correlation in the Northern Hemisphere (20°N_60°N). a) Geopotential height (500 hPa), b) Streamfunction (200 hPa), and c) Zonal component of the wind (850 hPa). Anomaly correlations are averaged over all model run cases in each phase of the MJO and Null cases (see text for details).
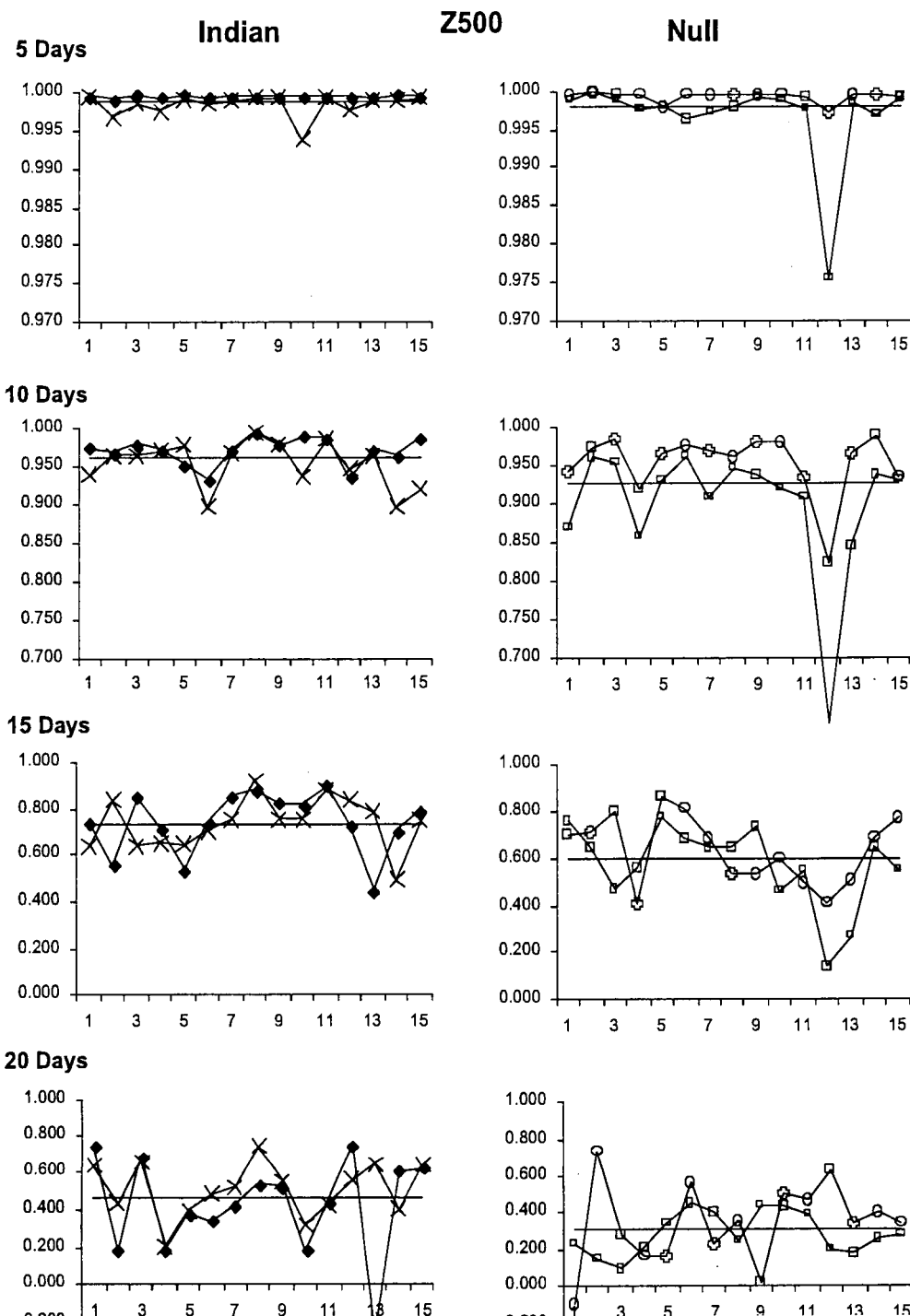
Figure 3. Boreal winter anomaly correlation of Z500 in the Northern Hemisphere (20°N_60°N). Anomaly correlations are shown for each model run experiment for active MJO in the Indian Ocean (left column) and Null cases (right column). Lead times are displayed from 5 to 20 days. Thick horizontal lines indicate the average of the anomaly correlation at the given lead time.
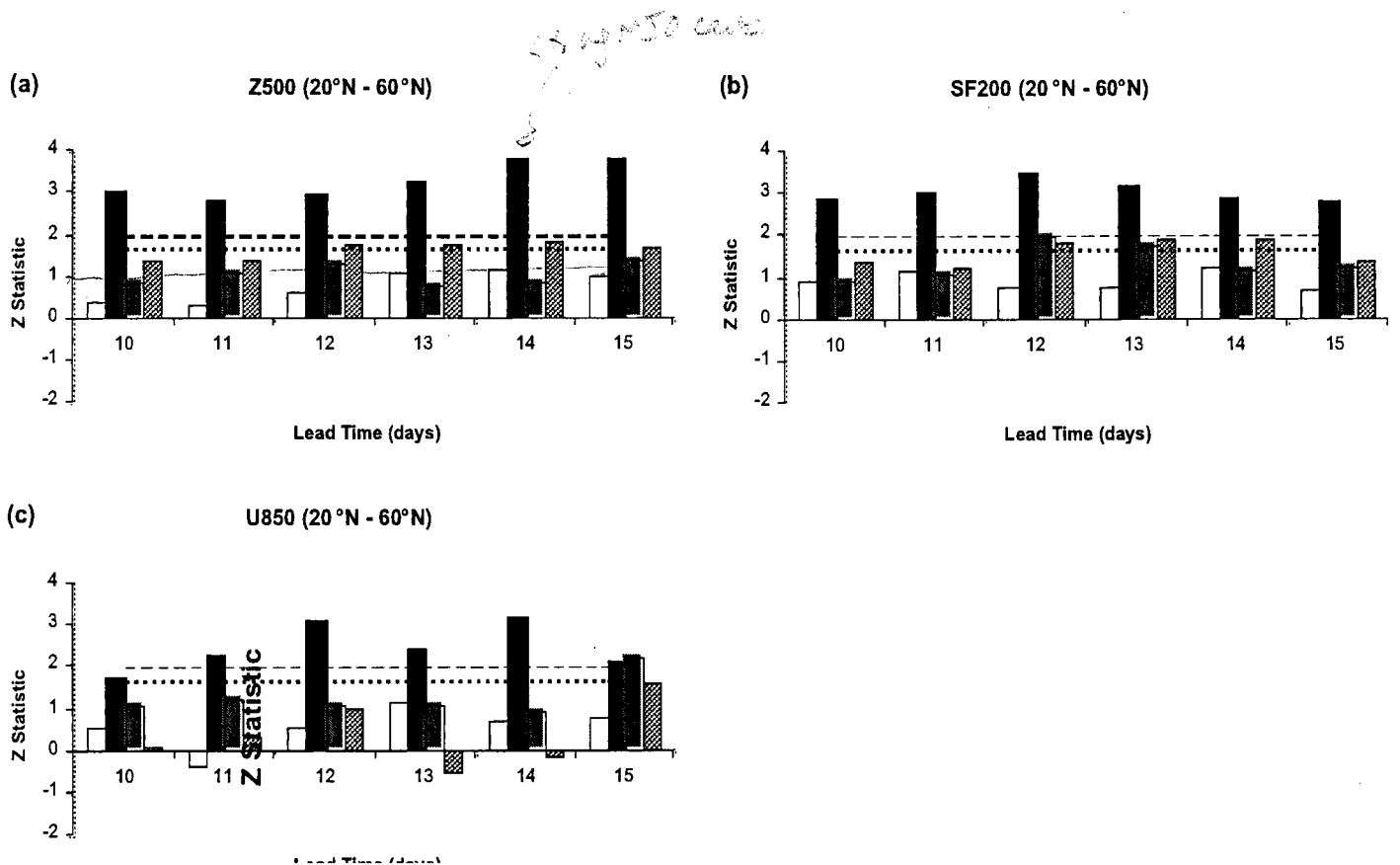
(a) Z500 (20°N - 60°N)

(b) SF200 (20°N - 60°N)

(c) U850 (20°N - 60°N)

Figure 4. *Z test* statistic of difference in boreal winter mean anomaly correlation between active MJO and Null situations. Short and long dash horizontal lines indicate 90% and 95% significance levels.
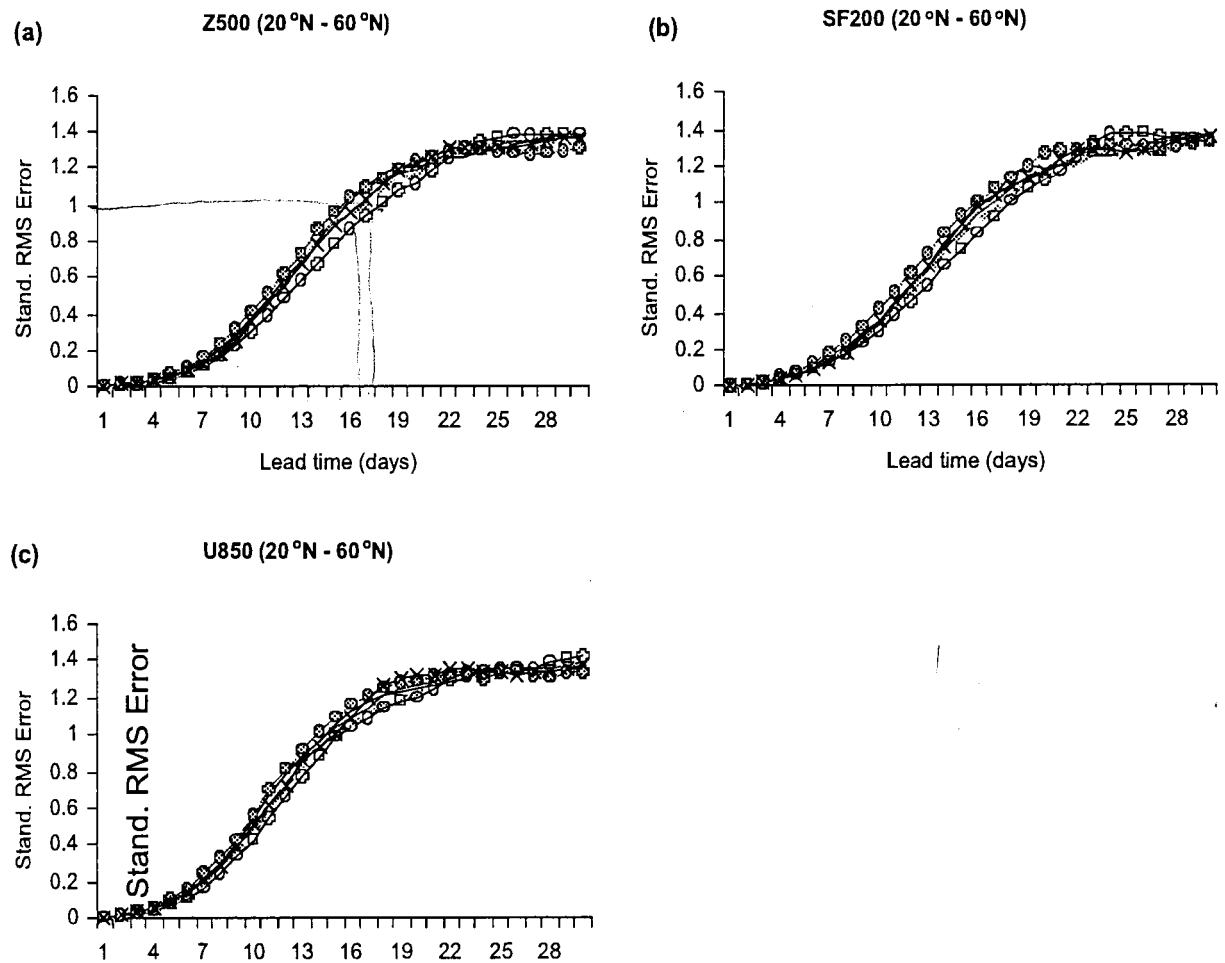
(a) Z500 (20°N - 60°N)

(b) SF200 (20°N - 60°N)

(c) U850 (20°N - 60°N)

Figure 5. Boreal winter mean standardized root-mean-square error (RMS) in the Northern Hemisphere (20°N_60°N). a) Geopotential height (500 hPa), b) Stream function (200 hPa), and c) Zonal component of the wind (850 hPa).
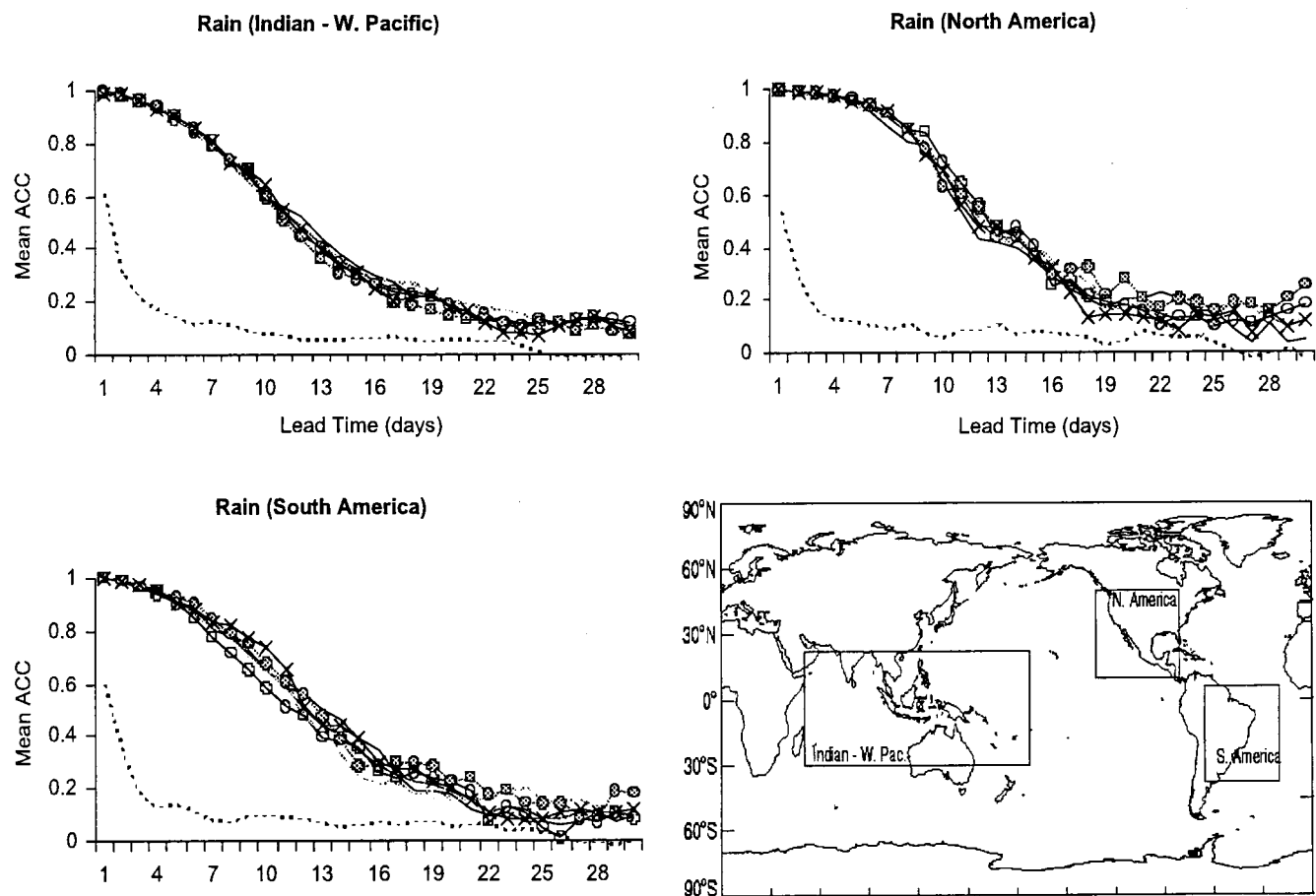
Figure 6. Boreal winter mean anomaly correlation of rainfall. Anomaly correlations are computed in the three regions indicated on the bottom right and averaged over all model run cases in each phase of the MJO and Null cases.

Popular Summary

The Madden and Julian Oscillation (MJO) is the most important atmospheric variability in the tropical atmosphere, on time scales from 20-90 days. While the sources of variability is in the tropics, the influences of the MJO is global. It is the most basic atmospheric phenomenon that determines the feasibility of extended range weather, or short-term climate forecasts, in many regions of the world, including the Asian-Australian monsoon, the monsoons of Americas and Africa, , as well as regions in the extratropics such as west coasts of North and South America. Correctly simulating the MJO in climate models is a challenging problem. The Goddard Laboratory for Atmospheres (GLA)/SUNY GCM is among a handful of models in the world that simulates reasonably well the MJO. This paper presents results of the impacts of the MJO on weather predictability in the northern hemisphere during the boreal winter using the GLA/SUNY GCM. Results indicate that during active periods the limit of useful prediction may be extended by 3-5 days, compared to quiescent periods of the oscillation.